



Title:

Parametric Modeling and Simulation of a Simplified Horizontal Tail Under the Framework of Iso-geometric Analysis

Authors:

Xiaoxiao Du, duxiaoxiao@buaa.edu.cn, Beihang University
 Gang Zhao, gangzhao@tsinghua.edu.cn, Tsinghua University
 Wei Wang, jrrt@buaa.edu.cn, Beihang University
 Yazui Liu, liyuzui@buaa.edu.cn, Beihang University
 Pengfei Zhang, ftd423@buaa.edu.cn, Beihang University
 Pengfei Han, hanpf@buaa.edu.cn, Beihang University
 He Cheng, naler@163.com, Beihang University

Keywords:

Parametric Modeling, Iso-geometric Analysis, Horizontal Tail, Multiple NURBS patches, Mindlin Shell

DOI: 10.14733/cadconfP.2023.132-137

Introduction:

The tail structure, also called the stabilizers, in the conventional aircraft configuration is normally arranged at the rear of the fuselage, providing for trim, stability and control [6,10]. It primarily consists of the horizontal tail and the vertical tail as shown in Fig. 1. The horizontal tail looks like a little wing and is utilized to balance the aircraft by creating a lift force, which is significant to the safety of an aircraft. A horizontal tail structure generally includes ribs, spars, skins and stringers which are assembled with mechanical fasteners. In this paper we develop a unified framework for designing and analyzing simplified horizontal tails based on iso-geometric analysis [5], which is considered to be an advanced numerical method from the perspective of CAD/CAE integration. When some basic parameters are given, a horizontal tail can be modeled automatically. Meanwhile the number of ribs, spars and their layout could also be regarded as design variables. The designed model can be simulated directly using the iso-geometric method under the developed framework.

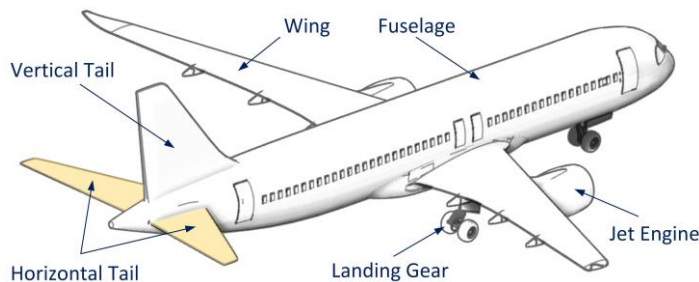


Fig. 1: A conventional aircraft configuration and the main parts definitions.

Horizontal Tail Geometry:

The geometry parameters of the horizontal tail are preliminarily given as: tail span $b = 12.70$ m, aspect ratio $A_R = 4.04$, taper ratio $T_R = 0.26$, back-ward quarter chord sweep $\Lambda_{1/4} = 30^\circ$, dihedral angle $\theta = 7^\circ$.

Assume that the planform of the horizontal tail is linearly tapered as shown in Fig. 2, then the tail reference area S_W can be expressed as [6]:

$$S_W = \frac{b^2}{A_R} = \frac{1}{2} C_R + C_T \cdot b, \quad (2.1)$$

where the parameters C_R and C_T denote the root chord and tip chord of the horizontal tail, respectively. According to the above equation and predefined parameters, we can easily obtain that $C_R = 4.9899 \text{ m}$ and $C_T = 1.2973 \text{ m}$. Given a reference coordinate system, the relative positions of the root chord and tip chord could be defined by the quarter chord sweep.

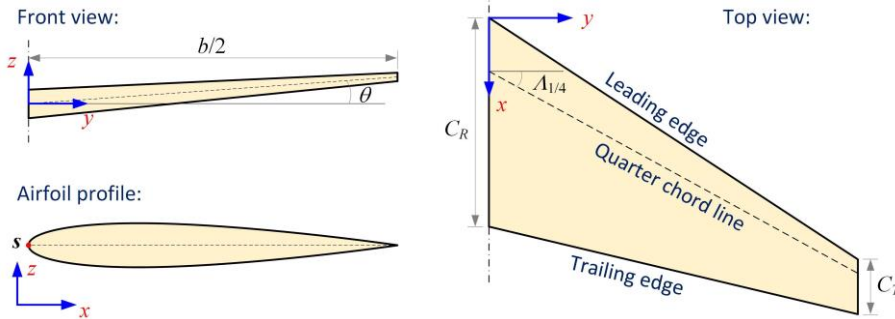


Fig. 2: The top view, front view and airfoil profile of a horizontal tail.

As for the airfoil profile of the horizontal tail, we choose the symmetrical NACA-0012 type airfoil, which could be explicitly defined by the formula as [8]:

$$z_i \ x = 0.5 \cdot t \cdot C \left[0.2969 \sqrt{\frac{x}{C}} - 0.1260 \left(\frac{x}{C} \right) - 0.3516 \left(\frac{x}{C} \right)^2 + 0.2843 \left(\frac{x}{C} \right)^3 - 0.1015 \left(\frac{x}{C} \right)^4 \right], \quad (2.2)$$

in which $x \in [0, C]$ and C is the chord length. The calculated z_i indicates the half thickness of the airfoil at the coordinate x . The parameter t denotes the maximum half thickness and is defined by the last two digits in the NACA 4-digits denomination divided by 100. For example, t takes value 0.12 to the type NACA-0012.

Parametric Modeling:

To avoid dealing with trimming and stitching problems in IGA [2,11], we utilize multiple conforming NURBS patches to build the horizontal tail, which is divided into three parts: ribs, spars and skins. In the following, we will discuss the parametric modeling of these parts in detail.

Rib Modeling

Ribs are used to provide the shape and thickness of the tail and are spaced along the tail span direction. Assume that the number of the ribs is adjustable and only three spars are designed as depicted in Fig. 3. Let n_r be the number of ribs and they are equally spaced along the span direction. The first rib and the end rib are located at the root and the tip of the tail. Then the distance between the i -th rib and the aircraft centerline is expressed as

$$d_i = \frac{b}{2 n_r - 1} i, \quad i = 0, 1, \dots, n_r - 1. \quad (3.1)$$

For the i -th rib, its chord length C_i could be linearly interpolated from C_R and C_T , written as

$$C_i = C_R - \frac{2 C_R - C_T}{b} d_i = C_R - \frac{C_R - C_T}{n_r - 1} i. \quad (3.2)$$

When the chord length C_i is obtained, its structural dimensions could be computed with Eqn. (2.2). Note that NURBS possesses affine invariance property, we can build NURBS patches for a normalized rib structure and map them to specific positions. The global coordinates of the left endpoint S , for the i -th rib, as given in Fig. 2, could be expressed as

$$S_i \ x, y, z = \left[\frac{1}{4} C_R - C_i + d_i \tan \Lambda_{1/4}, \ d_i, \ d_i \tan \theta \right]. \quad (3.3)$$

Generally, the rib structure is designed with holes to reduce weight. Figure 3 shows an example of the rib structure for the designed horizontal tail. The blue lines denote the spars and the red curve denotes the airfoil profile. Two holes are designed and radius $r = t \cdot C/6$ and $R = t \cdot C/4$.

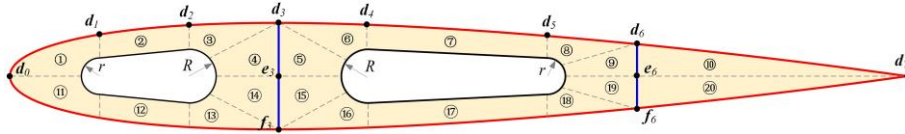


Fig. 3: A rib structure of the horizontal tail and its quad-domain segmentation.

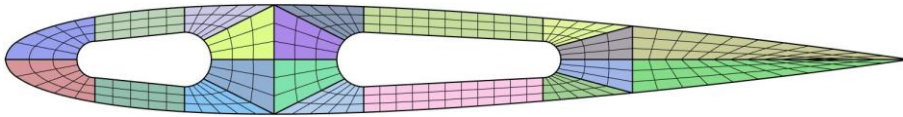


Fig. 4: The rib structure is built with 20 conforming NURBS patches.

For multi-patch modeling, the rib structure should be first divided into conforming quad subdomains as depicted in Fig. 3, where dotted lines denote the interfaces of subdomains. Each sub-domain is further re-constructed with a single NURBS patch. The airfoil profile is expressed by an explicit function as given in Eqn. (2.2) and should be re-expressed by a series of NURBS curves. In this paper the LSPIA method [1,7] is used to fit the airfoil profile. According to the domain segmentation, the airfoil profile is divided into seven segments for curve fitting as shown in Fig. 3. The endpoints are labeled as d_i ($i = 0, 1, 2, \dots, 7$).

To construct the patch $\textcircled{1}$, as labeled in Fig. 3, we ought to fit the curve segment $d_0 d_1$, which is discretized into $m+1$ data points Q_j ($j = 0, 1, 2, \dots, m$). Using the classical chord length parameterization method [9], the data point Q_j is assigned a parameter u_j . Let $n+1$ and P be the number and coordinates of control points, then the fitting curve at the k -th iteration could be generated as

$$C^k \ u = \sum_{i=0}^n P_i^k R_i \ u. \quad (3.4)$$

At the $(k+1)$ -th iteration, the control points are updated by [1]

$$P_i^{k+1} = P_i^k + \Delta_i^k, \quad \Delta_i^k = \mu \sum_{j=0}^m R_i \ u_j \ \delta_j^k, \quad \delta_j^k = Q_j - C^k \ u_j, \quad (3.5)$$

in which μ is a constant and is recommended to take the value $2/M$ [1]. Let m_i be the sum of the i -th row elements of $A^T A$ and $M = \max(m_i)$. A is a collocation matrix, written as

$$A_{m+1 \times n+1} = \begin{bmatrix} R_0 \ u_0 & R_1 \ u_0 & \cdots & R_n \ u_0 \\ R_0 \ u_1 & R_1 \ u_1 & \cdots & R_n \ u_1 \\ \vdots & \vdots & \ddots & \vdots \\ R_0 \ u_m & R_1 \ u_m & \cdots & R_n \ u_m \end{bmatrix}. \quad (3.6)$$

The iteration process is terminated when the fitting error is lower than the given tolerance. The obtained fitting curve is served as one of the boundary curves of the patch $\textcircled{1}$. The circular curve

segment of the left hole could be exactly represented by a NURBS curve, which is also served as one of the boundary curves. Then the patch ① can be obtained by linearly interpolating these two boundary curves. Similarly, we can construct all the other patches. The final construction of the rib consists of 20 NURBS patches and is illustrated in Fig. 4. Note that the patches ⑩ and ⑳ are degenerated at the right shape edge.

Spar Modeling

There are two spars designed in the horizontal tail. The blue lines given in Fig. 3 are the intersections of spars and ribs, denoted by $\mathbf{d}_3\mathbf{f}_3$ and $\mathbf{d}_6\mathbf{f}_6$. For conforming modeling, each spar between adjacent ribs is constructed with two NURBS patches. The curve segments $\mathbf{d}_3\mathbf{e}_3$ and $\mathbf{e}_3\mathbf{f}_3$ belong to different patches. The coordinates of point \mathbf{d}_3 in the local system are represented by $[0.3C, z_i(0.3C)]$. For the i -th rib, the global coordinates of the point \mathbf{d}_3 could be represented by

$$\mathbf{d}_3^i = \mathbf{S}_i + [0.3C_i, 0, z_i, 0.3C_i], \quad (3.7)$$

where z_i is calculated by Eqn. (2.2) and \mathbf{S}_i is given in Eqn. (3.3). The global coordinates of the points \mathbf{e}_3 and \mathbf{f}_3 can be easily recovered from \mathbf{d}_3 . In the same way, point \mathbf{d}_6 can be obtained by substituting the coefficient 0.3 given in Eqn. (3.7) with 0.7. These two position coefficients can also be regarded as design variables.

When the corner points of each spar are calculated, we can construct the intersection lines coincided with the rib structure and linearly interpolate the intersection lines between adjacent ribs. Eventually, two spars are built with $4(n-1)$ NURBS patches.

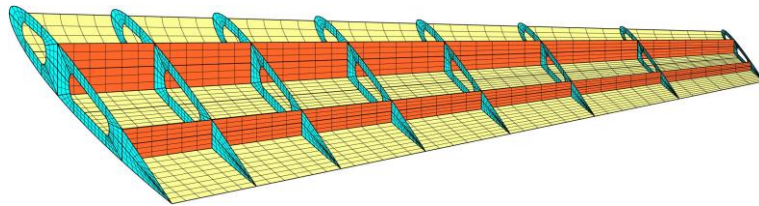


Fig. 5: The structural layout of the horizontal tail consisting of 8 ribs, 2 spars and 2 skins. Each rib is built with 20 NURBS patches. Each spar is built with 14 NURBS patches and each skin is built with 49 NURBS patches.

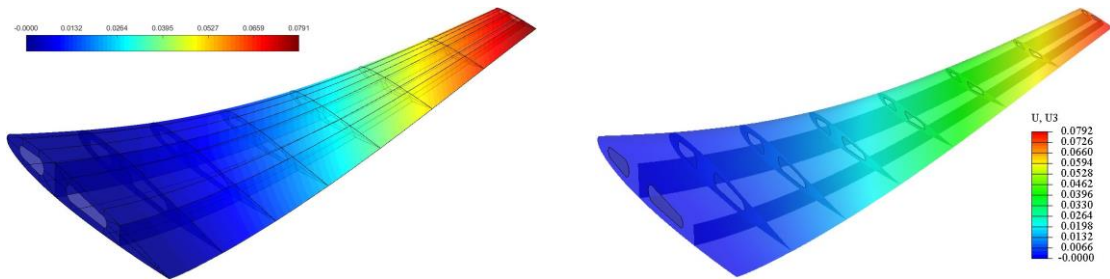


Fig. 6: The contour plots of vertical displacement of the horizontal tail obtained by using (a) iso-geometric method and (b) finite element method. The deformation scaling factor takes the value 30.

Skin Modeling

The skin can be divided into the upper and bottom parts. They can further be modeled by interpolating the adjacent rib profiles. Therefore, there are $n-1$ skin segments and each skin segment is a ruled surface. According to the segmentation of the airfoil profile given in Fig. 3, the upper part of the profile is divided into 7 curve segments. As a consequence, the upper skin part between adjacent ribs is construed by 7 NURBS patches. Then whole skin model will include $14(n-1)$ NURBS patches.

Figure 5 shows a designed example of the horizontal tail, which consists of 8 ribs, 2 spars and 2 skins. Each rib is built with 20 NURBS patches and is rendered in cyan. Each spar is built with 14 NURBS patches and is rendered in orange. Each skin is built with 49 NURBS patches and is rendered in light yellow. Only the bottom skin part is visualized for better observing the inner structures. There is a total of 286 NURBS patches used for representing the horizontal tail model. For the tail with n_r ribs, the number of NURBS patches should be $38n_r - 18$.

Numerical verification:

In this section, we will test the linear elastic performance of the designed horizontal tail under the framework of iso-geometric analysis. The classical Mindlin shell theory with 6 DOF for each node is used. The thickness of all the tail structure sections is set as $h = 0.05m$ and the aluminum alloy 2024-T3 is assigned to each part with Young's modulus of $E = 73.4GPa$, Poisson's ratio of $\nu = 0.33$, the density of $\rho = 2780 kg/m^3$. The upper skin is subjected to a uniformly distributed upward force with the magnitude of $T = 1 \times 10^5 N$. The whole horizontal tail model is discretized into 7140 bi-quadratic elements for iso-geometric analysis. The contour plot of the obtained vertical displacement is given in Fig. 6(a) based on the open-source library NLIGA [3,4]. For comparison, the problem is also solved by using the commercial software Abaqus with 69342 STRI65 elements and the result is shown in Fig. 6(b). It can be found that both results agree very well. The maximum vertical displacements obtained by using IGA and FEA are $0.0791m$ and $0.0792m$, respectively.

Conclusions:

We developed an iso-geometric framework for parametric modeling and analyzing the aircraft's horizontal tail. Given some necessary geometry parameters, the tail could be automatically constructed by a series of conforming NURBS patches. Additionally, the tail structure could be adaptively modified according to the number of ribs. The iso-geometric Mindlin shell is employed to study the mechanical performance of the tail and the obtained results are verified by comparing them with FEA results.

Acknowledgments:

The work is supported by National Natural Science Foundation of China (Project Nos. 62102012, 52175213, 61972011 and 62002004) and Young Elite Scientists Sponsorship Program by CAST (Project No. 2022QNR001).

References:

- [1] Deng, C.; Lin, H.: Progressive and iterative approximation for least squares B-spline curve and surface fitting, *Computer-Aided Design*, 47, 2014, 32-44. <http://dx.doi.org/10.1016/j.cad.2013.08.012>
- [2] Du, X.; Zhao, G.; Wang, W.; Fang, H.: Nitsche's method for non-conforming multipatch coupling in hyperelastic isogeometric analysis, *Computational Mechanics*, 65(3), 2020, 687-710. <https://doi.org/10.1007/s00466-019-01789-x>
- [3] Du, X.; Zhao, G.; Wang, W.; Guo, M.; Zhang, R.; Yang, J.: NLIGA: A MATLAB framework for nonlinear isogeometric analysis, *Computer Aided Geometric Design*, 80, 2020, 101869. <https://doi.org/10.1016/j.cagd.2020.101869>
- [4] Du, X.; Zhao, G.; Zhang, R.; Wang, W.; Yang, J.: Numerical implementation for isogeometric analysis of thin-walled structures based on a Bézier extraction framework: nligaStruct, *Thin-Walled Structures*, 180, 2022, 109844. <https://doi.org/10.1016/j.tws.2022.109844>
- [5] Hughes, T. J.; Cottrell, J. A.; Bazilevs, Y.: Isogeometric analysis: CAD, finite elements, NURBS, exact geometry and mesh refinement, *Computer methods in applied mechanics and engineering*, 194(39-41), 2005, 4135-4195. <https://doi.org/10.1016/j.cma.2004.10.008>
- [6] Kundu, A. K., Price, M. A., & Riordan, D.: *Conceptual Aircraft Design: An Industrial Approach*, John Wiley & Sons, Hoboken, NJ, 2019.
- [7] Lin, H.; Maekawa, T.; Deng, C.: Survey on geometric iterative methods and their applications, *Computer-Aided Design*, 95, 2018, 40-51. <https://doi.org/10.1016/j.cad.2017.10.002>
- [8] Moran, J.: *An introduction to theoretical and computational aerodynamics*, John Wiley & Sons, New York, NY, 2003.

- [9] Piegl L; Tiller W.: The NURBS book, 2nd ed, Springer-Verlag, New York, NY, 1997.
- [10] Raymer, D.P.: Aircraft design: a conceptual approach, 6th ed, American Institute of Aeronautics and Astronautics, Inc., Reston, VA, 2018.
- [11] Zhao, G.; Du, X.; Wang, W.; Liu, B.; Fang, H.: Application of isogeometric method to free vibration of Reissner-Mindlin plates with non-conforming multi-patch, Computer-Aided Design, 82, 2017, 127-139. <https://doi.org/10.1016/j.cad.2016.04.006>